

## Model of a Raft in Both Leaves of an Asymmetric Lipid Bilayer

Roie Shlomovitz and M. Schick\*

Department of Physics, University of Washington, Seattle, Washington

**ABSTRACT** We present a theory of inhomogeneities in the plasma membrane, or rafts, that can exist in both leaves of the plasma membrane. We note that although neither of the major phospholipid components of the outer leaf, sphingomyelin (SM) nor phosphatidylcholine (PC), evinces a tendency to form phases characterized by nonzero curvature, one of the major components of the inner leaf, phosphatidylethanolamine (PE), displays a strong tendency to do so whereas the other, phosphatidylserine (PS), does not. Therefore, we posit that the concentration difference of PS and PE couples to height fluctuations of the plasma membrane bilayer. This brings about a microemulsion in the inner leaf. Coupling of the concentration difference between PS and PE in the inner leaf and SM and PC in the outer leaf propagates the microemulsion to that leaf as well. The characteristic size of the inhomogeneities is equal to the square-root of the ratio of the bending modulus of the bilayer to its surface tension, a size which is  $\sim 100$  nm for the plasma membrane. If the coupling between leaves were to be provided by the interchange of cholesterol, then our model raft would consist of SM and cholesterol in the outer leaf and PS and cholesterol in the inner leaf floating in a sea of PC and PE in both leaves.

### INTRODUCTION

The raft hypothesis, that the plasma membrane is heterogeneous, with regions preferentially linked to or occupied by proteins, has received enormous attention (1,2). These regions are believed to be dynamic and small; estimates range from as little as 10 to perhaps a few hundred nanometers (3,4). The hypothesis has been supported by a great deal of indirect, experimental evidence that has recently been the subject of an excellent review (5). Despite the evidence, the hypothesis remains controversial (6,7). One reason for this is, presumably, that the experimental evidence is indirect. Another is that the physical basis for such heterogeneities in the plasma membrane is unclear.

The most common rationale is that rafts are a consequence of macroscopic phase separation of plasma membrane lipids into two liquid phases (8). One phase is composed primarily of saturated lipid such as sphingomyelin (SM) and cholesterol, and is denoted liquid-ordered. The other is composed primarily of unsaturated lipid such as phosphatidylcholine (PC), and is denoted liquid-disordered (9). Such a hypothesis is consistent with the observation that symmetric bilayers composed of ternary mixtures of saturated and unsaturated lipids and cholesterol undergo liquid-liquid phase separation (10–13). Were such macroscopic phase separation to occur at biological temperatures in the plasma membrane, rafts could be identified with regions of one phase floating in a sea of the other. However, macroscopic phase separation is not observed in the plasma membrane. This failure has been ascribed to effects of the cytoskeleton (14), or to active processes (15). It could also be the case that the temperature of transition to two-phase

coexistence is lower than biologically relevant ones. Thus, it has also been hypothesized that rafts are the dynamic fluctuations associated with the critical point of that transition (16).

As emphasized by Devaux and Morris (17), any such interpretation faces a major difficulty in the fact that the compositions of the two leaflets of the plasma membrane are very different. Almost all of the SM is found in the outer leaflet where it constitutes  $\sim 0.42$  mol fraction of all phospholipids in that leaf. In the inner leaf, however, the SM mol fraction of phospholipids is only  $\sim 0.04$ , so that this leaf is almost entirely composed of unsaturated lipid (18). For this reason, it is not surprising that a symmetric bilayer whose composition mimics that of the inner leaf of the plasma membrane does not exhibit any tendency to undergo phase separation (19). Although coupling of the SM-rich outer leaf to the SM-poor inner leaf can result in a transition to coexisting phases in the bilayer (20,21), not only is the transition temperature lower than that in a symmetric, SM-rich bilayer, but the inner SM-poor leaf bilayer can express only little contrast between coexisting phases and little preferential partitioning of proteins. The same would be true of the inhomogeneities associated with critical composition fluctuations. Hence, as a conveyor of information from one side of the plasma membrane to the other (the function for which rafts were initially hypothesized), this sort of raft would not serve.

A second rationale was motivated by the experimental indications that rafts are small and dynamic. It posits that the two-dimensional system of lipids in the plasma membrane bears a resemblance to the well-studied bulk three-dimensional system of oil, water, and amphiphile, which can produce a microemulsion—a liquid phase characterized by small, dynamic, oil-rich and water-rich regions (22). The

Submitted April 15, 2013, and accepted for publication June 27, 2013.

\*Correspondence: [schick@phys.washington.edu](mailto:schick@phys.washington.edu)

Editor: Paulo Almeida.

© 2013 by the Biophysical Society  
0006-3495/13/09/1406/8 \$2.00

<http://dx.doi.org/10.1016/j.bpj.2013.06.053>



microemulsion is brought about by the addition of the amphiphile to the oil and water that effectively reduces to zero the interfacial tension between them. This results in an amount of interface between these regions that is proportional to the concentration of amphiphile, and therefore scales like the volume of the system rather than as its area, as in ordinary, macroscopic phase separation. One immediate problem with the idea that the plasma membrane is a microemulsion is that there is no obvious amphiphile. Therefore, it has been suggested that the common unsaturated biological lipids, which have one saturated and one unsaturated tail, could serve both as a component of a liquid-disordered phase and as an amphiphile, reducing the line tension between liquid-disordered and liquid-ordered phases (23–25). However a second problem is, once again, the lack of contrast between such phases in the inner leaf.

Recently, one of us (26) noted that the lack of an obvious amphiphile was not necessarily a difficulty to bringing about a microemulsion, because any process that tends to reduce the interfacial tension between regions of different composition could serve as well. There are many such processes, as discussed by Seul and Andelman (27). It was suggested that the process relevant to the plasma membrane was the coupling of fluctuations of curvature of the bilayer to fluctuations of its composition (28–30). A variant of this idea, that the coupling of composition fluctuations is to monolayer curvature, has recently been explored (31). Both mechanisms were, however, applied to symmetric bilayers and so, for the reasons given above, could not, in this form, be applied to the very asymmetric plasma membrane.

It is the purpose of this article to present a microemulsion-based theory of rafts—rafts that can be produced in an asymmetric lipid bilayer, and can exist in both of its leaves. We begin by recalling that the major phospholipids of the outer leaflet are SM and PC. The mol fractions of these two lipids are ~0.42 and 0.40 (18). The spontaneous curvature of these two lipids are similar, with that of SM being smaller than that of PC (32). Thus, it is not to be expected that fluctuation in their relative composition will couple strongly to fluctuations in bilayer curvature. On the other hand, the major components of the inner leaflet are phosphatidylethanolamine (PE) and phosphatidylserine (PS) with mol fractions of 0.44 and 0.30, respectively (18). The tendencies of these two lipids to display curvature differ significantly. This difference is manifest in their abilities to form inverted hexagonal phases, which PE does readily (33) in contrast to PS at physiological pH (34). Specific values of a lipid's spontaneous curvature depend, of course, on the length of the hydrocarbon tails, the number of double bonds, and the nature of the linkage of the tails to the backbone, acyl ester or alkyl ether (35). However, a specific example will suffice to indicate the general difference; the spontaneous curvature of DOPS

is  $+6.9 \times 10^{-2} \text{ (nm)}^{-1}$ , whereas that of DOPE is  $-33.3 \times 10^{-2} \text{ (nm)}^{-1}$  (36), some five times larger and of the opposite sign. Because of this large difference in the tendency to form structures with nonzero curvature, we posit that fluctuations in bilayer curvature couple to the relative concentrations of these major components of the inner leaf. We show that this can bring about a microemulsion in it consisting of charged PS-rich regions and of neutral PE-rich regions. The characteristic size of these regions is  $\lambda \approx (\kappa/\gamma)^{1/2}$ , where  $\kappa$  is the bending modulus of the bilayer and  $\gamma$  its surface tension. We then consider the effect of a coupling between these composition fluctuations and those between SM and PC in the single phase outer leaf. We know, of course, that these lipids do have a tendency to phase-separate, although we assume that they are not macroscopically phase-separated at biological temperatures. We show that the coupling between the leaves can bring about a microemulsion in the outer leaf as well, so that the microemulsion exists in both leaves. We conclude with a brief discussion of the coupling between leaves. Were it due to the exchange of cholesterol, then a reasonable picture of the resulting raft would be that of regions rich in SM and cholesterol in the outer leaf and of negatively-charged PS and cholesterol in the inner leaf floating in a sea of PC and PE in both leaves (Fig. 1). Because of the relatively large fraction of the raft components in their respective leaves, such a raft could have sufficient contrast in composition to function.

## METHODS

To reiterate, our basic idea is that the coupling of fluctuations in the bilayer height couples to differences in the mol fractions of PS and PE in the inner leaf; that this coupling can produce a microemulsion in the inner leaf; and that coupling of the inner and outer leaves can propagate the microemulsion to the outer leaf as well, where it will be manifest in local differences of the composition of SM and PC. We let the local difference in mol fraction of PS and PE be denoted  $\phi(r)$ , and that of SM and PC be denoted  $\psi(r)$ . We do not consider the role of cholesterol explicitly except as a possible agent that couples the two leaves, as will be discussed briefly later.

If there are  $N$  lipids in the inner leaf and  $N$  in the outer leaf, and the area of each leaf is  $A$ , then the local, planar, free energy functional per unit area of the bilayer can be written in the usual form (30)

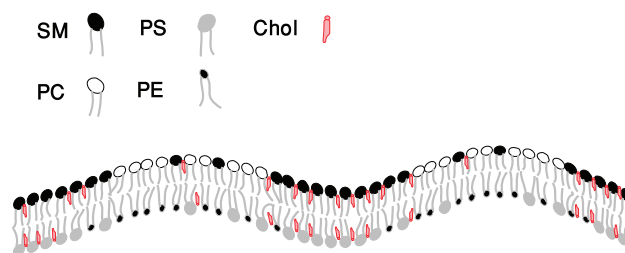


FIGURE 1 Regions rich in SM and cholesterol in the outer leaf and of negatively-charged PS and cholesterol in the inner leaf floating in a sea of PC and PE in both leaves.

$$\begin{aligned}
f_{\text{plane}}[\phi(\mathbf{r}), \psi(\mathbf{r})] = & -J_\phi n \phi^2 + \frac{k_B T}{2} n [(1 + \phi) \ln(1 + \phi) \\
& + (1 - \phi) \ln(1 - \phi)], \\
& -J_\psi n \psi^2 + \frac{k_B T}{2} n [(1 + \psi) \ln(1 + \psi) \\
& + (1 - \psi) \ln(1 - \psi)], \\
& -\Lambda \phi \psi,
\end{aligned} \quad (1)$$

where  $J_\phi < J_\psi$  are interaction energies,  $\Lambda$  is the strength of coupling between the leaves,  $n \equiv N/A$  is the areal density of lipids,  $k_B$  is Boltzmann's constant, and  $T$  the temperature. The total free energy of the planar bilayer is then

$$F_{\text{plane}}[\phi, \psi] = \int d^2 r \left[ \frac{b_\phi}{2} (\nabla \phi)^2 + \frac{b_\psi}{2} (\nabla \psi)^2 + f_{\text{plane}} \right], \quad (2)$$

where  $b_\phi$  is related to the line tension between regions rich in PS and those rich in PE, and  $b_\psi$  is similarly related to the line tension between regions rich in SM and those rich in PC. In this article, we will assume  $b_\phi = b_\psi$ .

The curvature free energy of the bilayer is taken to be (37)

$$F_{\text{curv}}[h] = \int d^2 r \left[ \frac{\kappa}{2} (\nabla^2 h)^2 + \frac{\gamma}{2} (\nabla h)^2 \right], \quad (3)$$

where  $h(r)$  is the height of the bilayer from some reference plane and  $\kappa$  and  $\gamma$  are the bilayer bending modulus and surface tension, respectively. The latter is the tension related to the membrane's response to normal, i.e., perpendicular to the membrane, strain (38,39). It is often referred to as the frame tension. For our purposes, we note that it is the quantity that can be obtained from tether-pulling experiments.

Lastly, we assume that the curvature of the bilayer couples to the difference in mol fractions of PS and PE in the inner leaflet:

$$F_{\text{coupl}}[\phi, h] = -\Gamma \int d^2 r (\nabla^2 h) \phi. \quad (4)$$

The total free energy,  $\tilde{F}_{\text{tot}}[\phi, \psi, h]$  is then  $\tilde{F}_{\text{tot}} = F_{\text{plane}} + F_{\text{curv}} + F_{\text{coupl}}$ .

The dependence of the free energy on height  $h$  can be eliminated, as  $\tilde{F}_{\text{tot}}$  depends only quadratically on  $h$ . To do so, we write  $\tilde{F}_{\text{tot}}$  in the space of Fourier transforms

$$\begin{aligned}
\tilde{F}_{\text{tot}} = & \int d^2 r f_{\text{plane}} + \frac{A^2}{(2\pi)^2} \int d^2 k \left[ \frac{b_\psi}{2} k^2 \psi(k) \psi(-k) \right. \\
& + \frac{b_\phi}{2} k^2 \phi(k) \phi(-k) + \frac{1}{2} [\kappa k^4 + \gamma k^2] h(k) h(-k) \\
& \left. + \Gamma k^2 h(k) \phi(-k) \right],
\end{aligned} \quad (5)$$

$$\phi(k) = \frac{1}{A} \int (\phi(r) - \bar{\phi}) e^{-ikr} d^2 r$$

and similarly for  $\psi(k)$ , with  $\bar{\phi}$  and  $\bar{\psi}$  the average values of  $\phi(\mathbf{r})$  and  $\psi(\mathbf{r})$ ,

$$\bar{\phi} \equiv \frac{1}{A} \int d^2 r \phi(\mathbf{r}),$$

$$\bar{\psi} \equiv \frac{1}{A} \int d^2 r \psi(\mathbf{r}).$$

Minimizing  $\tilde{F}_{\text{tot}}$  with respect to  $h(-k)$ , one obtains

$$h(k) = -\frac{\Gamma \phi(k)}{\kappa k^2 + \gamma}.$$

Substitution into Eq. 5 yields

$$\begin{aligned}
F_{\text{tot}}[\phi, \psi] = & \int d^2 r f_{\text{plane}} + \frac{A^2}{(2\pi)^2} \int d^2 k \left[ \frac{b_\psi}{2} k^2 \psi(k) \psi(-k) \right. \\
& \left. + \frac{b_\phi}{2} \left\{ 1 - \frac{(\Gamma^2/b_\phi \gamma)}{1 + \kappa k^2/\gamma} \right\} k^2 \phi(k) \phi(-k) \right].
\end{aligned} \quad (6)$$

We are most interested in the disordered, fluid phase, for which the ensemble average values of all quantities are constant, independent of position. To examine the fluctuations in that phase, we expand  $\phi(r)$ ,  $\psi(r)$  about their average values  $\bar{\phi}$  and  $\bar{\psi}$ , and then expand the free energy,  $F_{\text{tot}}[\phi, \psi]$ , about that of the uniform fluid phase to second order in these deviations. The result is (40)

$$\begin{aligned}
F_{\text{tot}}[\phi, \psi] = & F_{\text{tot}}(\bar{\phi}, \bar{\psi}) + \frac{A^2}{(2\pi)^2} \int d^2 k \\
& \times \left[ \left\{ a_\phi + \frac{b_\phi}{2} \left[ 1 - \frac{(\Gamma^2/b_\phi \gamma)}{(1 + \kappa k^2/\gamma)} \right] k^2 \right\} \phi(k) \phi(-k) \right. \\
& \left. + \left( a_\psi + \frac{b_\psi}{2} k^2 \right) \psi(k) \psi(-k) - \Lambda \phi(k) \psi(-k) \right],
\end{aligned} \quad (7)$$

where

$$a_\phi = \frac{n}{2} \left[ \frac{k_B T}{1 - \bar{\phi}^2} - 2J_\phi \right],$$

$$a_\psi = \frac{n}{2} \left[ \frac{k_B T}{1 - \bar{\psi}^2} - 2J_\psi \right].$$

The quantity  $a_\psi$ , with the dimension of energy per unit area, measures how far the temperature  $T$  is from the critical temperature,  $2J_\psi/k_B$ , of a symmetric, uncoupled (i.e.,  $\Lambda = 0$ ), bilayer with equal average compositions of SM and PC ( $\bar{\psi} = 0$ ). A similar statement applies to  $a_\phi$ .

The nature of the fluid phase is manifest in the structure functions  $S_{\phi\phi} \equiv \langle \phi(k) \phi(-k) \rangle$ ,  $S_{\psi\psi} \equiv \langle \psi(k) \psi(-k) \rangle$ , and  $S \equiv \langle \phi(k) \psi(-k) + \psi(k) \phi(-k) \rangle / 2$ , which are all measurable, in principle, by means of scattering. The brackets denote an ensemble average. The structure functions are most easily calculated in the representation in which the quadratic form of Eq. 7 is diagonal. The results are (24,41)

$$S_{\phi\phi} = \frac{2g_\psi}{4g_\phi g_\psi - \Lambda^2}, \quad (8)$$

$$S_{\psi\psi} = \frac{2g_\phi}{4g_\phi g_\psi - \Lambda^2}, \quad (9)$$

$$S_{\phi\psi} = \frac{\Lambda}{4g_\phi g_\psi - \Lambda^2}, \quad (10)$$

where

$$g_\phi(k) = \Lambda \left\{ \frac{(b_\phi/2\Lambda)(\kappa/\gamma)k^4 - (b_\phi/2\Lambda)[(\Gamma^2/b_\phi\gamma) - 1]k^2}{1 + \kappa k^2/\gamma} + \frac{a_\phi}{\Lambda} \right\}. \quad (11)$$

$$g_\psi(k) = \Lambda \left\{ \frac{b_\psi}{2\Lambda}k^2 + \frac{a_\psi}{\Lambda} \right\}. \quad (12)$$

## RESULTS

The phase diagram of our model, as obtained below, depends directly on three intensive parameters: the temperature,  $T$ ; the strength,  $\Gamma$ , of the coupling between curvature fluctuations and the composition of the inner leaf; and  $\Lambda$ , the strength of the coupling between compositions of the inner and outer leaves. This latter coupling has been estimated by May (42), utilizing theoretical arguments of Collins (43), to be such that  $0.1 < \Lambda/nk_B T < 1.0$ . We choose the lower limit and can display the diagram in the plane of temperature,  $T$ , and dimensionless coupling,  $\Gamma/(b_\phi\gamma)^{1/2}$ . For convenience, we will discuss the system in which the average values of the composition differences,  $\bar{\phi}$  and  $\bar{\psi}$ , are zero. Because the relative amounts of SM and PC in the outer leaf of the plasma membrane are comparable, as are the relative amounts of PS and PE in the inner leaf, this is a particularly interesting situation to examine. The phase diagram is shown in Fig. 2 *a*.

There are four distinct phases: Fluid, liquid-ordered, liquid-disordered, and modulated.

For any coupling and at sufficiently high temperature, there is first a fluid phase. It is characterized by the vanishing of the ensemble average of all Fourier components of the order parameters. As the temperature is lowered, for small values of the coupling  $\Gamma$ , a critical point is encountered below which the system separates into two uniform fluid phases, denoted 2 in Fig. 2 *a*, whose compositions differ from the averages taken over the entire bilayer; that is, in one phase,  $\langle\phi(k=0)\rangle$  and  $\langle\psi(k=0)\rangle$  are  $>0$ , whereas in the other  $\langle\phi(k=0)\rangle$  and  $\langle\psi(k=0)\rangle$  are  $<0$ . The former would be identified with the liquid-ordered phase, and the latter with the liquid-disordered one. The critical point temperature can be obtained from the fact that the three structure functions, evaluated at  $k=0$ , diverge at the critical point. Therefore it is located by setting  $4g_\phi(0)g_\psi(0) - \Lambda^2 = 4a_\phi a_\psi - \Lambda^2$  to zero. This yields

$$k_B T_c(J_\phi, J_\psi, \Lambda) = J_\phi + J_\psi + \left[ (J_\phi - J_\psi)^2 + \left(\frac{\Lambda}{n}\right)^2 \right]^{1/2}. \quad (13)$$

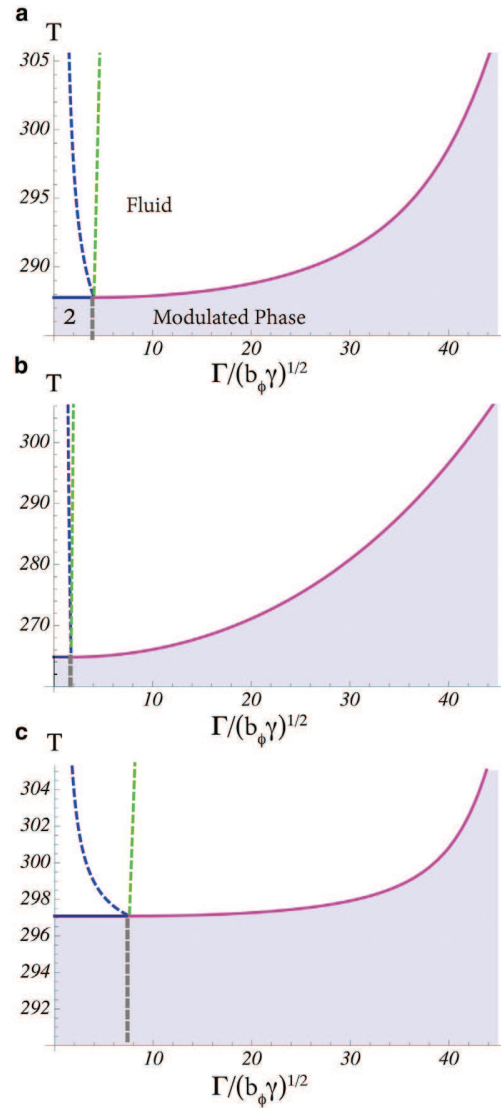


FIGURE 2 Phase diagrams of the system for three different couplings between the leaves. Each diagram exhibits four phases: For any coupling  $\Gamma$ , there is at sufficiently high temperatures a fluid phase; at lower temperatures and small  $\Gamma$ , the system separates into two fluid phases, liquid-ordered and liquid-disordered (this region is denoted 2 in the diagram); and at sufficiently large  $\Gamma$ , a modulated phase occurs. In the fluid phase: (leftmost dashed line) Lifshitz line of  $S_{\phi\phi}$ ; (rightmost dashed line) Lifshitz line of  $S_{\psi\psi}$ . (a)  $\Delta/nk_B T = 0.1$ , (b)  $\Delta/nk_B T = 0.5$ , and (c)  $\Delta/nk_B T = 0.05$ . The figures are plotted using  $T_c(J_\psi, J_\psi, \Lambda) = 300$  K,  $T_c(J_\phi, J_\phi, \Lambda) = 200$  K,  $b_\phi = b_\psi = 5 k_B T$ ,  $n^{-1} = 0.5 \text{ nm}^2$ ,  $\bar{\phi} = \bar{\psi} = 0$ , and  $(\kappa/\gamma)^{1/2} \approx 100$  nm.

We have chosen the interaction strength  $J_\psi$  such that a symmetric bilayer with leaves of a composition mimicking that of the outer leaf of the plasma membrane would have a transition temperature  $T_c(J_\psi, J_\psi, \Lambda) = 300$  K. In light of numerous experiments on such symmetric bilayers (13), this is reasonable. For a symmetric bilayer with composition mimicking that of the inner leaf, we have chosen the interaction  $J_\phi$  such that this bilayer would have a transition temperature of  $T_c(J_\phi, J_\phi, \Lambda) = 200$  K. This is in accord with the

observed lack of phase separation in such a bilayer (44), and yields a critical point temperature for the asymmetric bilayer of 288 K that is not unreasonable.

In addition to the fluid, liquid-ordered, and liquid-disordered phases, there is at any temperature, for sufficiently large coupling  $\Gamma$ , a modulated, or stripe, phase which is characterized by nonzero values of the Fourier components  $\langle\phi(k)\rangle$  and  $\langle\psi(k)\rangle$  for  $k$  equal to integer multiples of a fundamental wavevector characterizing the pattern of stripes. (We note that thermal fluctuations significantly alter the properties of this phase, but it remains a thermodynamically distinct one (45). This is not of interest to us here.) In the approximation in which we have solved our model, the transition from the fluid phase to the modulated phase is also continuous. Hence, the structure functions also diverge at this transition; however, they do not diverge at  $k = 0$  but at a nonzero value,  $k^*$ . To determine  $k^*$  and  $T_c^{\text{stripe}}(\Gamma)$ , the line of transitions, we define the denominator of the structure functions,  $D(k) \equiv 4g_\phi(k)g_\psi(k) - \Lambda^2$ , and denote by  $k^*$  that value at which  $D(k)$  is minimum

$$\begin{aligned} \left. \frac{\partial D(k)}{\partial k} \right|_{k^*} &= 0, \\ \left. \frac{\partial^2 D(k)}{\partial k^2} \right|_{k^*} &> 0 \end{aligned} \quad (14)$$

and equal to zero,  $D(k^*) = 0$ . These two conditions determine  $T_c^{\text{stripe}}(\Gamma)$ , and the value of  $k^*$ .

The two lines of continuous transitions, one from the fluid phase to two-phase coexistence, the other from the fluid phase to the modulated phase, meet at a point, which is denoted the Lifshitz point (46). As it is approached along the second of these two lines,  $k^* \rightarrow 0$ , the wavelength of the stripe phase becomes infinitely large. Lastly, the liquid-ordered, liquid-disordered, and modulated phases coexist along a line of triple points shown schematically in the figure.

The fluid phase is of most interest to us. In the region of phase space in which the coupling  $\Gamma$  is not large, the fluid is an ordinary one, and by that we mean that the correlation function of the order parameters,  $\langle\phi(0)\phi(\mathbf{r})\rangle$  and  $\langle\psi(0)\psi(\mathbf{r})\rangle$ , decay exponentially on the scale of the correlation length  $\xi$ . The structure functions  $\langle\phi(k)\phi(-k)\rangle$  and  $\langle\psi(k)\psi(-k)\rangle$ , which are the Fourier transforms of the correlation functions and which, in principle, can be measured in scattering experiments, have a maximum in the limit of vanishing wavevector,  $k \rightarrow 0$ . This fluid is well characterized by the single length,  $\xi$ .

This simple description is not correct for larger couplings  $\Gamma$ . In a region of the  $T, \Gamma$  phase space near that of the modulated phase, the fluid phase can be viewed as a melted modulated phase. The modulated phase is characterized by translational order of some wavelength. The fluid, to which it melts, has no translational order so that all correlations decay exponentially with a correlation length  $\xi$ . However,

the forces which brought about a variation in composition in the modulated phase are still manifest in the fluid whose correlations oscillate in space with a wavelength  $\lambda$  but with an amplitude that decays exponentially; they are well approximated by the correlation function  $g = (r)^{-1/2}\exp(-r/\xi)\cos(2\pi r/\lambda)$ . Thus, the fluid is a structured one that is characterized by two lengths,  $\lambda$  and  $\xi$ , in contrast to a usual fluid phase characterized only by the correlation length. It is just this dependence on two lengths that identifies this fluid with structure as a microemulsion. Given the particular mechanism that produces this microemulsion, the coupling of bilayer height fluctuations to concentration differences, the characteristic length of  $\lambda$  and  $\xi$  is set by  $\sqrt{\kappa/\gamma}$ .

The boundary between the ordinary fluid and the microemulsion is an arbitrary one because the free energy passes smoothly between the two. A useful distinction is provided by the peak in the structure functions of Eqs. 8–10. As noted above, in an ordinary fluid, these functions are maximum at a vanishing value of  $k$ . In the microemulsion, however, the peak in these functions occur at a nonzero value of wavevector,  $k_{\text{max}}$ , which indicates structure in the fluid of characteristic size  $\lambda = 2\pi/k_{\text{max}}$ . The line  $T_{\text{Lif}}(\Gamma)$ , at which the peak moves off of a zero wavevector, is denoted the Lifshitz line (22), and serves as a useful boundary between usual fluid and microemulsion.

Each of the three different structure functions,  $S_{\phi\phi}$ ,  $S_{\phi\psi}$ , and  $S_{\psi\psi}$ , has its own Lifshitz line. Because it is the composition difference of the inner leaflet that couples most strongly to the height fluctuations, the function  $S_{\phi\phi}$  is expected to display the behavior of a microemulsion most readily. In the phase diagram of Fig. 2 a, the leftmost dashed line is the Lifshitz line of  $S_{\phi\phi}$ . The location of the peak in the structure function  $S_{\psi\psi}$  indicates whether the structure produced in the inner leaf is conveyed sufficiently strongly to the outer one that composition fluctuations there signal the presence of a microemulsion in that leaf as well. This need not be so. Because there is no thermodynamic singularity in the free energy to signal the distinction between normal fluid and microemulsion, it is possible for the outer leaf to behave as an ordinary fluid even though the inner leaf is a microemulsion. Such a system would not serve as an effective raft, however. In the phase diagram of Fig. 2 a, the rightmost dashed line is the Lifshitz line of  $S_{\psi\psi}$ . To the right of this line, both leaves of the bilayer are microemulsion and the bilayer would display raft behavior. For the coupled system with  $\Lambda/(nk_B T) = 0.1$ , the structure functions  $S_{\phi\phi}$  and  $S_{\psi\psi}$  are shown in Fig. 3 at a value of  $\Gamma/(b_\phi\gamma)^{1/2} = 32$ , a value obtained from an estimate given below, and which is deep within the microemulsion. Both functions display a maximum at a nonzero wavevector,  $k_{\text{max}}$ , indicative of a microemulsion in both leaves.

We note that the magnitude of the peak in the structure function describing the outer leaflet  $S_{\psi\psi}$ , is much larger than that of the peak in the structure function describing the inner leaflet,  $S_{\phi\phi}$ —indicating a much larger fluctuation

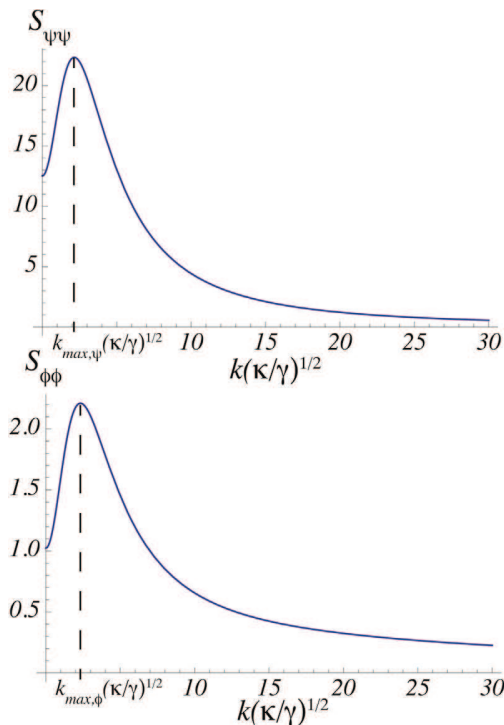


FIGURE 3 The structure functions  $S_{\psi\psi}$  and  $S_{\phi\phi}$  in the microemulsion region  $T = 310$ ,  $\Lambda = 0.1 nk_B T$ , and  $\Gamma/(b_\phi\gamma)^{1/2} = 32$ . All other parameters are the same as in Fig. 2.

response there despite the fact that the fluctuations in the height of the membrane couple directly to the order parameter of the inner leaf. The larger response in the outer leaf is simply due to the fact that the components in the outer leaf have a greater tendency to undergo phase separation than do the components of the inner leaf. Hence their susceptibility to thermal fluctuations is greater.

The probability that a bilayer is in a fluid microemulsion phase depends on the temperature and the couplings  $\Gamma$  and  $\Lambda$ . We discuss the coupling  $\Gamma$  first. An estimate (29,40) of the coupling between the bilayer curvature and the concentration difference of PS and PE is given by  $\Gamma = \kappa(c_{PS} - c_{PE})\alpha$ , where  $c_{PS} = 6.9 \times 10(\text{nm})^{-1}$  and  $c_{PE} = 33.3 \times 10(\text{nm})^{-1}$  are the spontaneous curvatures of DOPS and DOPE, respectively (36), and  $\alpha = 0.18$  is the average mol fraction of PS and PE in the bilayer. Using the measured value (47) of the bending modulus of a bilayer with cytoskeleton,  $\kappa = 270$  pN/nm, one finds that the coupling  $\Gamma = 108$  pN. To evaluate the dimensionless coupling,  $\Gamma/(b_\phi\gamma)^{1/2}$ , we use a typical value (48)  $b_\phi = 5k_B T = 20$  pN/nm and the measured surface tension of a bilayer with cytoskeleton (47)  $\gamma = 0.02$  pN/nm. We find, therefore, that the dimensionless coupling is  $\Gamma/(b_\phi\gamma)^{1/2} = 32$ . From Fig. 2 we see that this indicates that, if the bilayer is in a fluid phase, that fluid is most probably a microemulsion. At a temperature of  $T = 310$  and a coupling  $\Gamma/(b_\phi\gamma)^{1/2} = 32$ , the wavevector  $k_{\max}$  near which all the

structure functions would peak is  $k_{\max} = 3\sqrt{\gamma/\kappa}$ , which would lead to a raft size  $\lambda = 2\pi/k_{\max} = 243$  nm.

We turn now to the dimensionless coupling between leaves  $\Lambda/nk_B T$ . There are no experimental values of it, simply remarks about it. These include the observation that the coupling seems to transmit order from one leaf to the other, but does not affect the diffusion in them (20), and just the opposite observation (49). Further, the coupling is strong enough to align liquid-ordered domains across the two leaves of a symmetric bilayer (10,21). As noted earlier, May (42) estimated that  $\Lambda/nk_B T$  should be between 0.1 and 1.0, and it is for this reason that we have chosen the value  $\Lambda/nk_B T = 0.1$  in Fig. 2 a. If we take the larger value  $\Lambda/nk_B T = 0.5$ , then we obtain the phase diagram shown in Fig. 2 b. Note that for larger coupling between leaves,  $\Lambda$ , a smaller coupling to height fluctuations,  $\Gamma$ , is required to observe a microemulsion in both leaves. On the other hand, if we take the smaller value of  $\Lambda/nk_B T = 0.05$ , on the order obtained from a calculation of one particular form of coupling (50), we find the phase diagram of Fig. 2 c, which shows a larger phase space in which the inner leaf is a microemulsion whereas the outer leaf is not—a circumstance that would not lead to a functioning raft. Note that for this small value of  $\Lambda$ , a larger coupling  $\Gamma$  would be required to observe a microemulsion in both leaves.

## DISCUSSION

We have presented a theory that leads to composition inhomogeneities in both leaves of a lipid bilayer. What distinguishes it from almost all other theories of rafts in the plasma membrane is that the driving force is related to properties of the inner leaflet, in particular the difference in spontaneous curvatures of its major components, rather than to the tendency of the components in the outer leaflet to separate. The inhomogeneities are a characteristic of a microemulsion, a structured liquid, well studied in bulk amphiphilic systems, but rarely encountered in two-dimensional ones (51). Whereas other proposed mechanisms rely on some sort of amphiphile to bring about a microemulsion (23,24,52), ours utilizes the coupling of height fluctuations of the bilayer to the concentration fluctuations of the inner leaf. In contrast to theories that are based primarily upon the tendency of saturated and unsaturated lipids to undergo phase separation and which must therefore deal with the relative paucity of saturated lipids in the inner leaflet, our theory is based upon the architectural difference between two major components of the inner leaf, PS and PE. We have shown that formation of a microemulsion in the inner leaf can propagate to the outer leaf where it would be manifest in differences in concentration of SM and PC, the major components of that leaf. Of course such propagation of an effect from the inner to outer leaf depends upon the coupling,  $\Lambda$ , between leaves. We have seen that

a coupling of the order of magnitude expected theoretically is sufficient to produce a microemulsion in both leaves provided that the coupling  $\Gamma$  between the membrane height fluctuations and composition differences is strong enough. The value of this coupling is unknown, but again, theoretical estimates (26) indicate that it is of the necessary order of magnitude.

We note that the nature of the coupling between the leaves of the plasma membrane is unclear, although several mechanisms have been proposed (42,43). One particularly attractive mechanism is due to the fact that cholesterol can flip-flop rapidly between the two leaves, much more rapidly than the other lipids. Presumably it does so between the regions of greatest disorder (53), that of PC in the outer leaf and PE in the inner. Further cholesterol is known to prefer SM to PC and PS to PE (54), and would therefore tend to increase the order of the chains of SM and PS, leading to increased interdigitation between them and aligning them. May (42) has used a simple model to conclude that cholesterol flip-flop could not provide a coupling of the expected size. We use an equally simple model (see the Appendix) to argue that it can. If we are correct, then our model of a raft would be that of a region rich in SM and cholesterol in the outer leaf and PS and cholesterol in the inner leaf floating in a sea rich in PC and PE in both the outer and inner leaves. Again because of the relative abundance of SM and of PC in the outer leaf and of PS and PE in the inner, such a raft would be a functional one.

## APPENDIX

From Niu and Litman (54), we know that if we set the energy of cholesterol in a PC environment to be zero, then the energy of cholesterol in a SM environment is  $E_{SM}/k_B T = -2$ , in a PS environment  $E_{PS}/k_B T = -0.68$ , and in a PE environment  $E_{PE} = +1.2$ . To estimate the coupling due to cholesterol, we consider the following two cases:

In the first, we assume the regions to be misaligned as far as the cholesterol is concerned; a region of SM is opposite PE, which is isolated from a region of PC opposite PS. We assume that the cholesterol is evenly divided between these two regions, which contain equal numbers of phospholipids. The product  $\phi\psi = -1$  in these regions. In this case, the average energy is

$$\frac{E_2}{Nk_B T} = \frac{1}{2} \left( \frac{-2e^2 + 1.2e^{-1.2}}{e^2 + e^{-1.2}} \right) + \frac{1}{2} \left( \frac{-0.68e^{0.68}}{e^{0.68} + 1} \right) = -1.16.$$

In the second case, we align the regions so that a raft consisting of SM in the outer leaf opposite PS in the inner leaf, is isolated from a sea of PC in the outer leaf opposite PE in the inner. This is the configuration favored by cholesterol, and we assume all the cholesterol is in the raft. The product  $\phi\psi = 1$  in this region. The average energy per particle of this system is

$$\frac{E_1}{Nk_B T} = \left( \frac{-2e^2 - 0.68e^{0.68}}{e^2 + e^{0.68}} \right) = -1.72.$$

Because the coupling energy per particle is  $-\phi\psi\Delta n/k_B T$ ,  $\Delta$  can be estimated from the difference of these two energies:  $-2\Delta/nk_B T = 1.72 - (-1.16)$  or  $\Delta/nk_B T = 0.28$ .

M.S. thanks the following for useful and informative conversations: David Andelman, Haim Diamant, Hiroshi Shigamora, Jerry Feigensohn, Mary Kraft, Erwin London, Tom Lubensky, and Benoit Palmieri. R.S. and M.S. are both grateful to Lutz Maibaum and Sarah Keller and their groups for their interest and interaction.

The work of M.S. is supported by the National Science Foundation under grant No. DMR-1203282. R.S. acknowledges financial support from the Raymond and Beverly Sackler Foundation.

## REFERENCES

1. Simons, K., and E. Ikonen. 1997. Functional rafts in cell membranes. *Nature*. 387:569–572.
2. Brown, D. A., and E. London. 1998. Structure and origin of ordered lipid domains in biological membranes. *J. Membr. Biol.* 164:103–114.
3. Sheets, E. D., G. M. Lee, ..., K. Jacobson. 1997. Transient confinement of a glycosylphosphatidylinositol-anchored protein in the plasma membrane. *Biochemistry*. 36:12449–12458.
4. Pralle, A., P. Keller, ..., J. K. Hörber. 2000. Sphingolipid-cholesterol rafts diffuse as small entities in the plasma membrane of mammalian cells. *J. Cell Biol.* 148:997–1008.
5. Lingwood, D., and K. Simons. 2010. Lipid rafts as a membrane-organizing principle. *Science*. 327:46–50.
6. Munro, S. 2003. Lipid rafts: elusive or illusive? *Cell*. 115:377–388.
7. Hancock, J. F. 2006. Lipid rafts: contentious only from simplistic standpoints. *Nat. Rev. Mol. Cell Biol.* 7:456–462.
8. Schroeder, R., E. London, and D. Brown. 1994. Interactions between saturated acyl chains confer detergent resistance on lipids and glycosylphosphatidylinositol (GPI)-anchored proteins: GPI-anchored proteins in liposomes and cells show similar behavior. *Proc. Natl. Acad. Sci. USA*. 91:12130–12134.
9. Ipsen, J. H., G. Karlström, ..., M. J. Zuckermann. 1987. Phase equilibria in the phosphatidylcholine-cholesterol system. *Biochim. Biophys. Acta*. 905:162–172.
10. Dietrich, C., L. A. Bagatolli, ..., E. Gratton. 2001. Lipid rafts reconstituted in model membranes. *Biophys. J.* 80:1417–1428.
11. Samsonov, A. V., I. Mihalyov, and F. S. Cohen. 2001. Characterization of cholesterol-sphingomyelin domains and their dynamics in bilayer membranes. *Biophys. J.* 81:1486–1500.
12. Veatch, S. L., and S. L. Keller. 2002. Organization in lipid membranes containing cholesterol. *Phys. Rev. Lett.* 89:268101.
13. Veatch, S. L., and S. L. Keller. 2005. Seeing spots: complex phase behavior in simple membranes. *Biochim. Biophys. Acta*. 1746:172–185.
14. Kusumi, A., Y. Sako, and M. Yamamoto. 1993. Confined lateral diffusion of membrane receptors as studied by single particle tracking (nanovid microscopy). Effects of calcium-induced differentiation in cultured epithelial cells. *Biophys. J.* 65:2021–2040.
15. Fan, J., M. Sammalkorpi, and M. Haataja. 2010. Influence of nonequilibrium lipid transport, membrane compartmentalization, and membrane proteins on the lateral organization of the plasma membrane. *Phys. Rev. E Stat. Nonlin. Soft Matter Phys.* 81:011908–011915.
16. Machta, B. B., S. Papanikolaou, ..., S. L. Veatch. 2011. Minimal model of plasma membrane heterogeneity requires coupling cortical actin to criticality. *Biophys. J.* 100:1668–1677.
17. Devaux, P. F., and R. Morris. 2004. Transmembrane asymmetry and lateral domains in biological membranes. *Traffic*. 5:241–246.
18. Devaux, P., and A. Zachowski. 1994. Maintenance and consequences of membrane phospholipid asymmetry. *Chem. Phys. Lipids*. 73:107–120.
19. Wang, T. Y., R. Leventis, and J. R. Silvius. 2000. Fluorescence-based evaluation of the partitioning of lipids and lipidated peptides into liquid-ordered lipid microdomains: a model for molecular partitioning into “lipid rafts”. *Biophys. J.* 79:919–933.

20. Kiessling, V., J. M. Crane, and L. K. Tamm. 2006. Transbilayer effects of raft-like lipid domains in asymmetric planar bilayers measured by single molecule tracking. *Biophys. J.* 91:3313–3326.
21. Collins, M., and S. Keller. 2008. Tuning lipid mixtures to induce domains across leaflets of unsupported asymmetric bilayers. *Proc. Natl. Acad. Sci. USA.* 105:124–128.
22. Gompper, G., and M. Schick. 1994. Self-Assembling Amphiphilic Systems. Academic Press, San Diego, CA.
23. Yamamoto, T., R. Brewster, and S. Safran. 2010. Chain ordering of hybrid lipids can stabilize domains in saturated/hybrid/cholesterol lipid membranes. *Euro Phys. Lett.* 91:28002.
24. Hirose, Y., S. Komura, and D. Andelman. 2012. Concentration fluctuations and phase transitions in coupled modulated bilayers. *Phys. Rev. E Stat. Nonlin. Soft Matter Phys.* 86:021916.
25. Palmieri, B., and S. A. Safran. 2013. Hybrid lipids increase the probability of fluctuating nanodomains in mixed membranes. *Langmuir.* 29:5246–5261.
26. Schick, M. 2012. Membrane heterogeneity: manifestation of a curvature-induced microemulsion. *Phys. Rev. E Stat. Nonlin. Soft Matter Phys.* 85:031902–031904.
27. Seul, M., and D. Andelman. 1995. Domain shapes and patterns: the phenomenology of modulated phases. *Science.* 267:476–483.
28. Leibler, S. 1986. Curvature instability in membranes. *J. Phys.* 47:507–516.
29. Leibler, S., and D. Andelman. 1987. Ordered and curved meso-structures in membranes and amphiphilic films. *J. Phys.* 48:2013–2018.
30. Sunil Kumar, P. B., G. Gompper, and R. Lipowsky. 1999. Modulated phases in multicomponent fluid membranes. *Phys. Rev. E Stat. Phys. Plasmas Fluids Relat. Interdiscip. Topics.* 60(4 Pt B):4610–4618.
31. Meinhardt, S., R. L. Vink, and F. Schmid. 2013. Monolayer curvature stabilizes nanoscale raft domains in mixed lipid bilayers. *Proc. Natl. Acad. Sci. USA.* 110:4476–4481.
32. Byström, T., and G. Lindblom. 2003. Molecular packing in sphingomyelin bilayers and sphingomyelin/phospholipid mixtures. *Spectrochim. Acta A.* 59:2191–2195.
33. Seddon, J. M., G. Cevc, ..., D. Marsh. 1984. X-ray diffraction study of the polymorphism of hydrated diacyl- and dialkylphosphatidylethanolamines. *Biochemistry.* 23:2634–2644.
34. Hope, M. J., and P. R. Cullis. 1980. Effects of divalent cations and pH on phosphatidylserine model membranes: a  $^{31}\text{P}$  NMR study. *Biochem. Biophys. Res. Commun.* 92:846–852.
35. Lohner, K., A. Hermetter, and F. Paltauf. 1984. Phase behavior of ethanolamine plasmalogen. *Chem. Phys. Lipids.* 34:163–170.
36. Fuller, N., C. R. Benatti, and R. P. Rand. 2003. Curvature and bending constants for phosphatidylserine-containing membranes. *Biophys. J.* 85:1667–1674.
37. Safran, S. 1994. Statistical Thermodynamics of Surfaces, Interfaces, and Membranes. Addison-Wesley, Reading, PA.
38. Diamant, H. 2011. Model-free thermodynamics of fluid vesicles. *Phys. Rev. E Stat. Nonlin. Soft Matter Phys.* 84:061123–061127.
39. Farago, O., and P. Pincus. 2004. Statistical mechanics of bilayer membrane with a fixed projected area. *J. Chem. Phys.* 120:2934–2950.
40. Liu, J., S. Qi, ..., A. K. Chakraborty. 2005. Phase segregation on different length scales in a model cell membrane system. *J. Phys. Chem. B.* 109:19960–19969.
41. Gompper, G., and M. Schick. 1990. Lattice model of microemulsions. *Phys. Rev. B Condens. Matter.* 41:9148–9162.
42. May, S. 2009. Trans-monolayer coupling of fluid domains in lipid bilayers. *Soft Matter.* 5:3148–3156.
43. Collins, M. D. 2008. Interleaflet coupling mechanisms in bilayers of lipids and cholesterol. *Biophys. J.* 94:L32–L34.
44. Wang, T. Y., and J. R. Silvius. 2001. Cholesterol does not induce segregation of liquid-ordered domains in bilayers modeling the inner leaflet of the plasma membrane. *Biophys. J.* 81:2762–2773.
45. Toner, J., and D. Nelson. 1981. Smectic, cholesteric, and Rayleigh-Bernard order in two dimensions. *Phys. Rev. B.* 23:316–334.
46. Hornreich, R., M. Luban, and S. Shtrikman. 1975. Critical behavior at the onset of k-space instability along the  $\lambda$  line. *Phys. Rev. Lett.* 35:1678–1681.
47. Dai, J., and M. P. Sheetz. 1999. Membrane tether formation from blebbing cells. *Biophys. J.* 77:3363–3370.
48. Lipowsky, R. 1992. Budding of membranes induced by intramembrane domains. *J. Phys. II.* 2:1825–1840.
49. Chiantia, S., and E. London. 2012. Acyl chain length and saturation modulate interleaflet coupling in asymmetric bilayers: effects on dynamics and structural order. *Biophys. J.* 103:2311–2319.
50. Putzel, G., and M. Schick. 2011. Insights on raft behavior from minimal phenomenological models. *J. Phys. Condens. Matter.* 23:284101.
51. Spivak, B., and S. Kivelson. 2006. Transport in two dimensional electronic micro-emulsions. *Ann. Phys.* 321:2071–2115.
52. Brewster, R., P. A. Pincus, and S. A. Safran. 2009. Hybrid lipids as a biological surface-active component. *Biophys. J.* 97:1087–1094.
53. Risselada, H. J., and S. J. Marrink. 2008. The molecular face of lipid rafts in model membranes. *Proc. Natl. Acad. Sci. USA.* 105:17367–17372.
54. Niu, S.-L., and B. J. Litman. 2002. Determination of membrane cholesterol partition coefficient using a lipid vesicle-cyclodextrin binary system: effect of phospholipid acyl chain unsaturation and headgroup composition. *Biophys. J.* 83:3408–3415.